HHS Public Access

Author manuscript

Int J Cardiovasc Imaging. Author manuscript; available in PMC 2021 June 05.

Published in final edited form as:

Int J Cardiovasc Imaging. 2020 July ; 36(7): 1363–1370. doi:10.1007/s10554-020-01818-4.

Prevalence of mitral annular disjunction in patients with mitral valve prolapse and severe regurgitation

Andrew J. Putnam[1], **Kalie Kebed**[1], **Victor Mor-Avi**[1], **Nina Rashedi**[1], **Deyu Sun**[2], **Brooke Patel**[1], **Husam Balkhy**[1], **Roberto M. Lang**[1], **Amit R. Patel**[1]

[1]Biological Sciences Division, University of Chicago Medicine, Chicago, IL, USA

[2]Philips Healthcare, Andover, MA, USA

Abstract

Mitral annular disjunction (MAD) is routinely diagnosed by cardiac imaging, mostly by echocardiography, and shown to be a risk factor for ventricular arrhythmias. While MAD is associated with mitral valve (MV) prolapse (MVP), it is unknown which patients with MAD are at higher risk and which additional imaging features may help identify them. The value of cardiac computed tomography (CCT) for the diagnosis of MAD is unknown. Accordingly, we aimed to: (1) develop a standardized CCT approach to identify MAD in patients with MVP and severe mitral regurgitation (MR); (2) determine its prevalence and identify features that are associated with MAD in this population. We retrospectively studied 90 patients (age 63 ± 12 years) with MVP and severe MR, who had pre-operative CCT (256-slice scanner) of sufficient quality for analysis. The presence and degree of MAD was assessed by rotating the view plane around the MV center to visualize disjunction along the annulus. Additionally, detailed measurements of MV apparatus and left heart chambers were performed. Univariate logistic regression analysis was performed to determine which parameters were associated with MAD. MAD was identified in 18 patients (20%), and it was typically located adjacent to a prolapsed or flail mitral leaflet scallop. Of these patients, 75% had maximum MAD distance > 4.8 mm and 90% > 3.8 mm. Female gender was most strongly associated with MAD ($p = 0.04$). Additionally, smaller end-diastolic mitral annulus area ($p = 0.045$) and longer posterior leaflet ($p = 0.03$) were associated with greater MAD. No association was seen between MAD and left ventricular size and function, left atrial size, and papillary muscle geometry. CCT can be used to readily detect MAD, by taking advantage of the 3D nature of this modality. A significant portion of MVP patients referred for mitral valve repair have MAD. The presence of MAD is associated with female gender, smaller annulus size and greater posterior leaflet length.

Amit R. Patel, apatel2@medicine.bsd.uchicago.edu.

Electronic supplementary material The online version of this article (https://doi.org/10.1007/s10554-020-01818-4) contains supplementary material, which is available to authorized users.

Compliance with ethical standards

Conflicts of interest The authors declare that they have no competing interests.

Ethical approval All procedures performed in studies involving human participants were in accordance with the ethical standards of the institutional and/or national research committee and with the 1964 Helsinki declaration and its later amendments or comparable ethical standards.

Informed consent The study was approved by the Institutional Review Board.

Keywords

Mitral annular disjunction; Mitral valve prolapse; Cardiac computed tomography

Introduction

Mitral valve (MV) prolapse (MVP) is a common clinical entity that is generally associated with a favorable prognosis, although sudden cardiac death has been reported in patients with MVP and no other apparent cause for malignant arrhythmias [1]. Previous studies have suggested that mitral annular disjunction (MAD), in addition to bileaflet MVP and papillary muscle fibrosis, is associated with an increased risk of ventricular arrhythmias [2–4]. MAD is an abnormality of the mitral annulus, in which the posterior MV leaflet inserts into the left atrial wall, separate from the left ventricular myocardium, which is normally in contact with the mitral annulus [5, 6]. In MAD, it has been proposed that abnormal mitral annular dynamics due to a non-communicating posterior leaflet may be an integral part of the pathology leading to increased risk of arrhythmias [7, 8]. However, the exact nature of the abnormality in annular dynamics remains unclear, and there is little information that could aid in predicting outcomes in patients with MVP and concomitant MAD.

Cardiac imaging, mostly echocardiography and more recently cardiac magnetic resonance, has been used to diagnose MAD [5, 7, 9, 10]. Although cardiac computed tomography (CCT) may be particularly suited for this purpose because of its true 3D nature with isotropic voxels and high spatial resolution, there are currently no standardized CCT protocols for MAD assessment. As a result, the value of CCT in this context remains to be determined. Specifically, it is unknown which features depicted by any imaging modality may help identify which patients with MAD are at higher risk for developing ventricular arrhythmias. Accordingly, the objectives of this study were to develop a standardized CCT approach to assess for MAD and determine its prevalence in patients with MVP and severe mitral regurgitation (MR), as well as to identify imaging features associated with MAD in this patient population.

Methods

Patient selection

We retrospectively studied 90 consecutive patients (age 63 ± 12 years) with MVP (including flail segments) and severe MR referred for CCT prior to robotic MV repair from 2013 to 2019. Patients with prior valve replacement were excluded. Also, patients were excluded if their CT scans did not contain sufficient cardiac phases (16 of the 106 patients in the initial cohort). Demographic and clinical information was obtained from electronic medical records, including age, sex, resting heart rate, blood pressure, reported symptoms, history of atrial fibrillation or non-sustained ventricular tachycardia. Electrocardiograms were also analyzed for the presence of premature ventricular contractions, atrial fibrillation and inferior T-wave inversions.

Image acquisition

Imaging was performed using a 256-slice multidetector CT scanner (Revolution, GE Healthcare, Milwaukee, Wisconsin, n = 47; or Brilliance iCT, Philips Healthcare, Cleveland OH, USA, n = 43). For the GE scanner, the following parameters were used: detector configuration of 256 × 0.625 mm; detector array (z-axis) dimension of 160 mm; tube voltage of 100–120 kVp, auto-modulated tube current–time product (mAs); for the Philips iCT, the parameters were: slice configuration was 128 × 0.625 mm; tube voltage of 100–120 kVp; tube current–time product of 250–300 mAs.

A bolus tracking algorithm was used with a region of interest (ROI) placed in the descending thoracic aorta. Image acquisition began 5–7 s after a Hounsfield Unit (HU) threshold of 110 was detected. Axial images were obtained using a single heartbeat acquisition during a breath hold and images were reconstructed for all phases (0–100%) of a single R-R interval in 10% increments. Contrast enhancement was achieved with 90–120 cc Iohexol 350 (350 mg/mL, Omnipaque, GE Healthcare) at an infusion rate of 5 cc/sec, followed by 40–50 cc of normal saline flush. The mean dose-length-product (DLP) for the cardiac portions of the scan was 675 ± 375 mGy*cm, corresponding to a mean dose was 9.5 ± 5.3 mSV.

Image analysis

Using post-processing software (Vitrea version 6.7.4, Vital Images Inc., Toshiba Medical, Minnetonka, MN, USA), images were first displayed in an axial, coronal and sagittal planes. Using multiplanar reconstruction (MPR), short-axis and two long-axis views of the left ventricle were identified and used for analysis of chamber volumes. Left ventricular (LV) long axis was identified and adjusted so that only the left ventricle was included from the MV to the apex. Left ventricular end-diastolic and end-systolic volumes (EDV, ESV) and ejection fraction (EF) were automatically obtained. In addition, maximal left atrial volume was measured at ventricular end-systole.

Assessment of mitral valve apparatus

In the LV short-axis plane, at the MV level, prolapsed or flail scallops were identified using MPR of all phases displayed as a cine loop. The entire valve was investigated by medial to lateral scrolling through the short axis of the mitral valve perpendicular to the coaptation line, allowing for identification of A3/P3, A2/P2, and A1/P1 leaflets, respectively (Fig. 1). A leaflet was considered prolapsed if its body protruded into the left atrium during systole, but the tip was directed downward, toward the MV plane. Flail was diagnosed if the leaflet tip was directed upward toward the left atrium.

To assess the mitral annulus, the LV short-axis plane at the MV level was first visualized using MPR at both end-diastole and end-systole. Then, with the MV annulus plane identified, the MV annulus area was measured using planimetry (Fig. 2a–c). Thereafter, the distance between the heads of the papillary muscles was measured in an end-diastolic mid-ventricular short-axis view. The angle between the anteromedial and posterolateral papillary muscles was measured using the center of the ventricular cavity as a reference point (Fig. 2d). A 3-chamber view was used at a cardiac phase consistent with mid-diastole to measure leaflet length (Fig. 2e).

Identification of mitral annular disjunction

MPR was applied to the end-systolic phase to obtain a short-axis plane of the mitral valve with the aorta in the twelve o'clock position. Slab thickness was increased to 3.0 mm and images were analyzed using maximal intensity projection (MIP) and Inverse MIP filters to aid in identification of MAD. Long-axis cross-sections were then used to radially sweep through the entire posterior leaflet to determine the presence of MAD (Videos 1 and 2) and to measure the maximum MAD distance from the LV free wall (Fig. 3).

Reproducibility Analysis

To assess inter-measurement variability, a second reader blinded to all prior results, repeated measurements of MAD distance from the LV free wall in 10 patients. Variability was expressed in terms of intra-class correlation (ICC) and absolute difference between the pairs of repeated measurements in percent of their mean.

Statistical analysis

Continuous variables are presented as mean ± SD unless indicated otherwise. Univariate logistic regression was used to calculate the odds-ratio that reflects the extent to which each demographic or imaging parameter was associated with MAD. A p-value of < 0.05 was considered statistically significant for all analyses.

Results

Patient characteristics

Of the 90 patients included in the analysis, there were 23 (26%) women and 67 (74%) men. For the entire cohort, LV EF was 62 ± 9.6%, and EDV was 175 ± 35 mL. Patients were normotensive, did not have tachycardia, and 70% were symptomatic, including: dyspnea (42%), palpitations (23%), fatigue (21%), and chest discomfort (16%), while 30% were asymptomatic. 27% had a documented history of atrial fibrillation. MVP (without flail) was present in 81 (90%) of all patients, while isolated flail was present in 6 (6.7%), and a combination of MVP and flail was present in 3 (3.3%) of the patients.

Mitral annular disjunction

MAD was identified in 18 patients (20%), of whom 9 were female (39% of the 23 women) and 9 were male (13% of the 67 men). Table 1 shows the distribution of prolapsing and flail mitral leaflet scallops in these patients. The maximum MAD distance from the LV free wall was 5.5 mm (IQR: 4.8 to 8.3 mm and 10%−90% limits: 3.8 to 9.6 mm). MAD was always located adjacent to a prolapsing or flail scallop and often extended beyond a single scallop. Most frequently, it involved the P2 scallop (16/18, 89%), and in the majority of patients, extended to the adjacent P1 (9/18, 50%) and P3 (10/18, 56%) scallops. Univariate logistic regression showed significant associations with the presence of MAD for female gender ($p = 0.04$), smaller end-diastolic mitral annulus area ($p = 0.045$), and a longer posterior leaflet ($p = 0.03$). No other imaging parameter related to the mitral valve apparatus, such as left atrial size, left ventricular size and function, and papillary muscle geometry, were associated with the presence of MAD (Table 2).

Reproducibility

Repeated assessment of MAD by a second independent observer resulted in the diagnosis of MAD in 16/18 patients (89% inter-reader agreement). Repeated measurements of the maximum MAD distance from the LV free wall resulted in ICC value of 0.97 and inter-measurement variability of 9.0 ± 9.1%.

Discussion

This study was designed to develop a systematic method to detect MAD by CCT, to determine its prevalence and relationship to location of MVP, and to determine which imaging and demographic features are associated with its presence. Prior work has described CCT imaging techniques to assess the MV prior to surgery, focusing on the identification of the prolapsed segments and MV morphology [11], but no studies have examined the role of CCT in the identification of MAD associated with MVP. We found that in our patient cohort, MAD could be readily and reproducibly detected by CCT using MPR, and that in addition to the female gender, longer posterior mitral valve leaflet and a smaller end-diastolic mitral annular area were associated with the presence of MAD.

It is known that sudden cardiac death occurs in a small subset of patients with MVP [1–3, 12, 13]. MAD is of clinical importance because its presence, irrespective of concomitant MVP, has been associated with a higher burden of ventricular arrhythmias [10]. However, it remains unknown which patients with MVP are at a higher arrhythmogenic risk. Recent papers have suggested that fibrosis of the papillary muscles and infero-basal LV wall may be a nidus for of arrhythmia generation in patients with MVP [2, 14, 15]. It has been postulated that areas of MAD generate mechanical stress of the papillary muscles and ventricular endocardium, which over time could cause fibrosis in some patients [10].

We found that isotropic CCT data acquisition, which creates a 3D dataset of images, permits easy visualization of the MV in several different planes [16], lending itself to readily identify the presence of MAD. Rotating around the MV annulus in the short axis plane, while simultaneously viewing the planes created by MPR allows for complete assessment of the mitral annulus. Unlike echocardiography, CT is not limited to standardized views that may incompletely visualize portions of the mitral annulus.

In this study, we focused on patients with severe MR and MVP or a flail mitral leaflet referred for CCT as part of preoperative planning. In an effort to study a cohort with degenerative MV disease, patients with prior mitral valve repair or replacement or rheumatic mitral valve disease were excluded. MAD was present in 20% of our cohort. Other studies utilizing transthoracic echocardiography have reported MAD prevalence of 40–55% in patients with myxomatous MV disease and severe MR, but these were smaller cohorts of patients, and women accounted for ~ 50% of patients as opposed to our cohort, where women only comprised 26% of patients [17]. Regardless of these cohort differences, MAD has proven to be a common finding in this patient population.

The definition of MAD in the literature has been inconsistent. In this study, we defined the presence of MAD as attachment of the mitral valve leaflet to the left atrial wall, irrespective

of the distance from the mitral annulus. The usefulness of this definition remains to be confirmed in future studies. It is interesting to note that > 90% of our patients had a MAD distance of > 3.8 mm from the mitral annulus, while > 75% of patients had a MAD distance of > 4.8 mm. In addition to better understanding the full spectrum of MAD distance from the annulus, our study also revealed that MAD was typically located adjacent to the mitral leaflet scallop that either prolapsed or was flail. Additionally, we observed that the MAD often extended beyond just a single scallop along the posterior mitral annulus [13].

It was previously reported that MVP is predominantly associated with female gender [13]. It was formerly thought that women may be more likely to present with symptoms, creating a referral bias that would inflate the prevalence of MVP in women. Later studies ruled out this referral bias by studying community populations, such as the Framingham Heart Study patients, and showed that women do in fact have a higher prevalence of MVP [12]. However, the reason for MVP being more prevalent in women remains unknown. Interestingly, our cohort was 74% male, which is consistent with prior studies demonstrating that males with MVP are more likely to progress to severe MR requiring surgery [18]. Although in our study, the preponderance of patients undergoing mitral valve repair were men, women were much more likely to have MAD. The female predominance of MAD was also shown by Carmo et al. who evaluated 38 patients with myxomatous MV disease, identifying 21/38 (55%) with MAD, of which 61% were women [17].

In an attempt to understand MAD and its relationship to the MV apparatus, we measured several dimensions of the mitral annulus, the MV leaflets, the papillary muscles, left atrium and left ventricle. In this study, patients with a smaller end-diastolic mitral annulus area and a longer posterior leaflet were more likely to have MAD. No other parameter related to the mitral valve apparatus, such as change in mitral annular size, the distance or angle between papillary muscles, LV or left atrial size was associated with the presence of MAD. A longer posterior leaflet length could potentially lead to tethering of the papillary muscle over time, and it is plausible that this could facilitate papillary muscle tip and left ventricular endocardial fibrosis, which is believed to confer a higher risk of arrhythmias [2, 10, 14, 15]. Moreover, the tethering effects caused by the prolonged posterior mitral valve leaflet could be magnified by the presence of a smaller mitral annulus.

Considerable research has focused on patients with MVP with severe MR. If MAD is identified in a cohort of patients with milder MR, future studies should focus on patients with MAD who have only mild to moderate MR over an extended period of time to determine whether the degree of MAD is related to the severity of MR, whether MR severity worsens more rapidly compared to patients with MAD, and whether the risk of malignant arrhythmias changes with MR severity.

The primary clinical implication of our study is that an assessment for MAD should be considered to be part of the routine pre-surgical CCT examination of patients with MVP and severe MR. Given its association with ventricular arrhythmias, patients with MAD may require additional imaging to assess for fibrosis, or monitoring to assess arrhythmic burden.

Our study has several limitations. First, this is a retrospective single-center study which limits external validity. Second, our study was restricted to patients with MVP and severe MR referred for cardiac surgery. There may be many individuals with MVP and MAD who are asymptomatic and thus the true prevalence of MAD is difficult to assess. Also, it has been shown that MAD can exist without concomitant MVP, meaning that conclusions from our study may only be applicable to those patients with MAD and MVP. Moreover, in this retrospective study, we did not have a "gold standard" reference for the presence of MAD, because it was neither assessed during surgery nor reported in the surgeons' notes, and also intraoperative transesophageal echocardiogram was not targeted at detecting this pathology and therefore the existing images could not be used to provide confident determination with this regard. Finally, one of the challenges with MAD distance measurements is the determination whether it reflects the distance to the true atrial wall or atrial wall covered by a mitral leaflet plastered against the wall, in which case the MAD distance may be underestimated.

In conclusion, our findings suggest that MAD can be accurately diagnosed by analysis of CCT scans in patients with severe MR, by taking advantage of the 3D nature of this modality. MAD is common in patients with MVP complicated by severe MR. Its presence is associated with female gender, longer posterior leaflet length and smaller mitral annulus. Assessment for MAD should be included as part of the routine pre-surgical imaging of patients with MVP and severe MR.

Supplementary Material

Refer to Web version on PubMed Central for supplementary material.

Abbreviations

CCT	Cardiac computed tomography
EDV	End-diastolic volume
ESV	End-systolic volume
EF	Ejection fraction
LV	Left ventricular
MAD	Mitral annular disjunction
MPR	Multi-planar reconstruction
MR	Mitral regurgitation
MV	Mitral valve
MVP	Mitral valve prolapse

References

1. Nishimura RA, McGoon MD, Shub C, Miller FA Jr, Ilstrup DM, Tajik AJ (1985) Echocardiographically documented mitral-valve prolapse. Long-term follow-up of 237 patients. N Engl J Med 313:1305–1309 [PubMed: 4058522]
2. Basso C, Perazzolo Marra M, Rizzo S et al. (2015) Arrhythmic mitral valve prolapse and sudden cardiac death. Circulation 132:556–566 [PubMed: 26160859]
3. Nordhues BD, Siontis KC, Scott CG et al. (2016) Bileaflet mitral valve prolapse and risk of ventricular dysrhythmias and death. J Cardiovasc Electrophysiol 27:463–468 [PubMed: 26749260]
4. Perazzolo Marra M, Basso C, De Lazzari M et al. (2016) Morpho-functional abnormalities of mitral annulus and arrhythmic mitral valve prolapse. Circ Cardiovasc Imaging 9:e005030 [PubMed: 27516479]
5. Eriksson MJ, Bitkover CY, Omran AS et al. (2005) Mitral annular disjunction in advanced myxomatous mitral valve disease: echocardiographic detection and surgical correction. J Am Soc Echocardiogr 18:1014–1022 [PubMed: 16198877]
6. Bharati S, Granston AS, Liebson PR, Loeb HS, Rosen KM, Lev M (1981) The conduction system in mitral valve prolapse syndrome with sudden death. Am Heart J 101:667–670 [PubMed: 7223606]
7. Lee AP, Jin CN, Fan Y, Wong RHL, Underwood MJ, Wan S (2017) Functional implication of mitral annular disjunction in mitral valve prolapse: a quantitative dynamic 3D echocardiographic study. JACC Cardiovasc Imaging 10:1424–1433 [PubMed: 28528161]
8. Enriquez-Sarano M (2017) Mitral annular disjunction: the forgotten component of myxomatous mitral valve disease. JACC Cardiovasc Imaging 10:1434–1436 [PubMed: 28528160]
9. Konda T, Tani T, Suganuma N et al. (2017) The analysis of mitral annular disjunction detected by echocardiography and comparison with previously reported pathological data. J Echocardiogr 15:176–185 [PubMed: 28799132]
10. Dejgaard LA, Skjolsvik ET, Lie OH et al. (2018) The mitral annulus disjunction arrhythmic syndrome. J Am Coll Cardiol 72:1600–1609 [PubMed: 30261961]
11. Koo HJ, Yang DH, Oh SY et al. (2014) Demonstration of mitral valve prolapse with CT for planning of mitral valve repair. Radiographics 34:1537–1552 [PubMed: 25310416]
12. Freed LA, Levy D, Levine RA et al. (1999) Prevalence and clinical outcome of mitral-valve prolapse. N Engl J Med 341:1–7 [PubMed: 10387935]
13. Zuppiroli A, Rinaldi M, Kramer-Fox R, Favilli S, Roman MJ, Devereux RB (1995) Natural history of mitral valve prolapse. Am J Cardiol 75:1028–1032 [PubMed: 7747683]
14. Kitkungvan D, Nabi F, Kim RJ et al. (2018) Myocardial fibrosis in patients with primary mitral regurgitation with and without prolapse. J Am Coll Cardiol 72:823–834 [PubMed: 30115220]
15. Sriram CS, Syed FF, Ferguson ME et al. (2013) Malignant bileaflet mitral valve prolapse syndrome in patients with otherwise idiopathic out-of-hospital cardiac arrest. J Am Coll Cardiol 62:222–230 [PubMed: 23563135]
16. Dalrymple NC, Prasad SR, Freckleton MW, Chintapalli KN (2005) Informatics in radiology (infoRAD): introduction to the language of three-dimensional imaging with multidetector CT. Radiographics 25:1409–1428 [PubMed: 16160120]
17. Carmo P, Andrade MJ, Aguiar C, Rodrigues R, Gouveia R, Silva JA (2010) Mitral annular disjunction in myxomatous mitral valve disease: a relevant abnormality recognizable by transthoracic echocardiography. Cardiovasc Ultrasound 8:53 [PubMed: 21143934]
18. Mohty D, Orszulak TA, Schaff HV, Avierinos JF, Tajik JA, Enriquez-Sarano M (2001) Very long-term survival and durability of mitral valve repair for mitral valve prolapse. Circulation 104:I1–I7 [PubMed: 11568020]

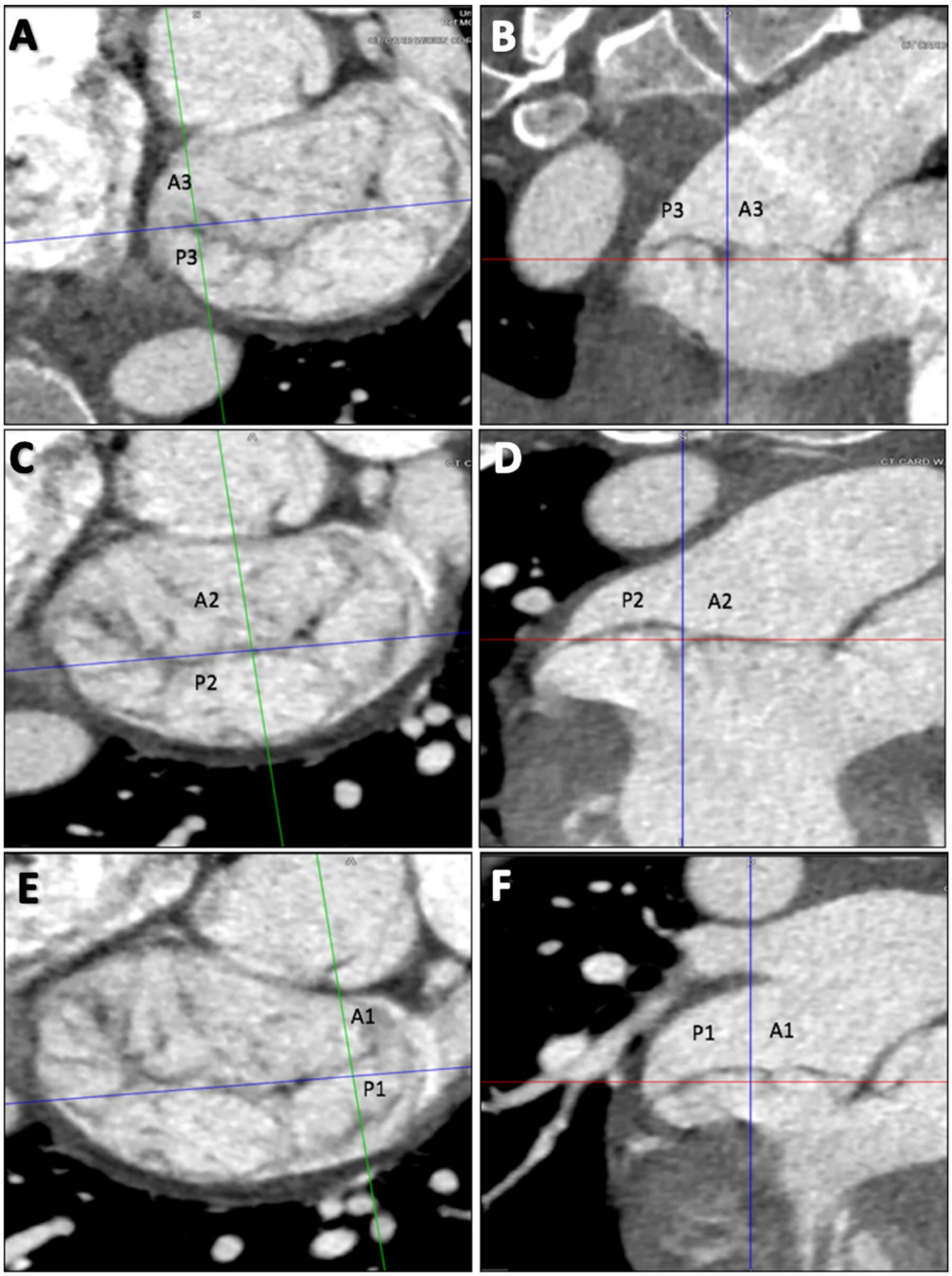

Fig. 1.

Three-chamber views at the level of mitral valve using multiplanar reconstruction to identify prolapse or flail leaflets. Starting with the medial aspect (**a**, **b**), the A3 and P3 scallops are identified. In the central portion of the MV (**c**, **d**), the A2 and P2 scallops are identified. When scrolling to the most lateral portion of the MV near the LAA (**e**, **f**), A1 and P1 are identified. In this example, there is P2 prolapse. MAD is also noted involving all three posterior scallops

Fig. 2.

Measuring the mitral annulus, papillary muscles, and leaflet length. The boundaries of the mitral annulus are outlined using arrows (**a**, **b**), then using planimetry, the MV area is measured in short axis (**c**). The distance and angle between the two papillary muscles is measured in the short axis (**d**). Anterior and posterior leaflet lengths are measured in the 3-chamber view in mid-diastole (**e**)

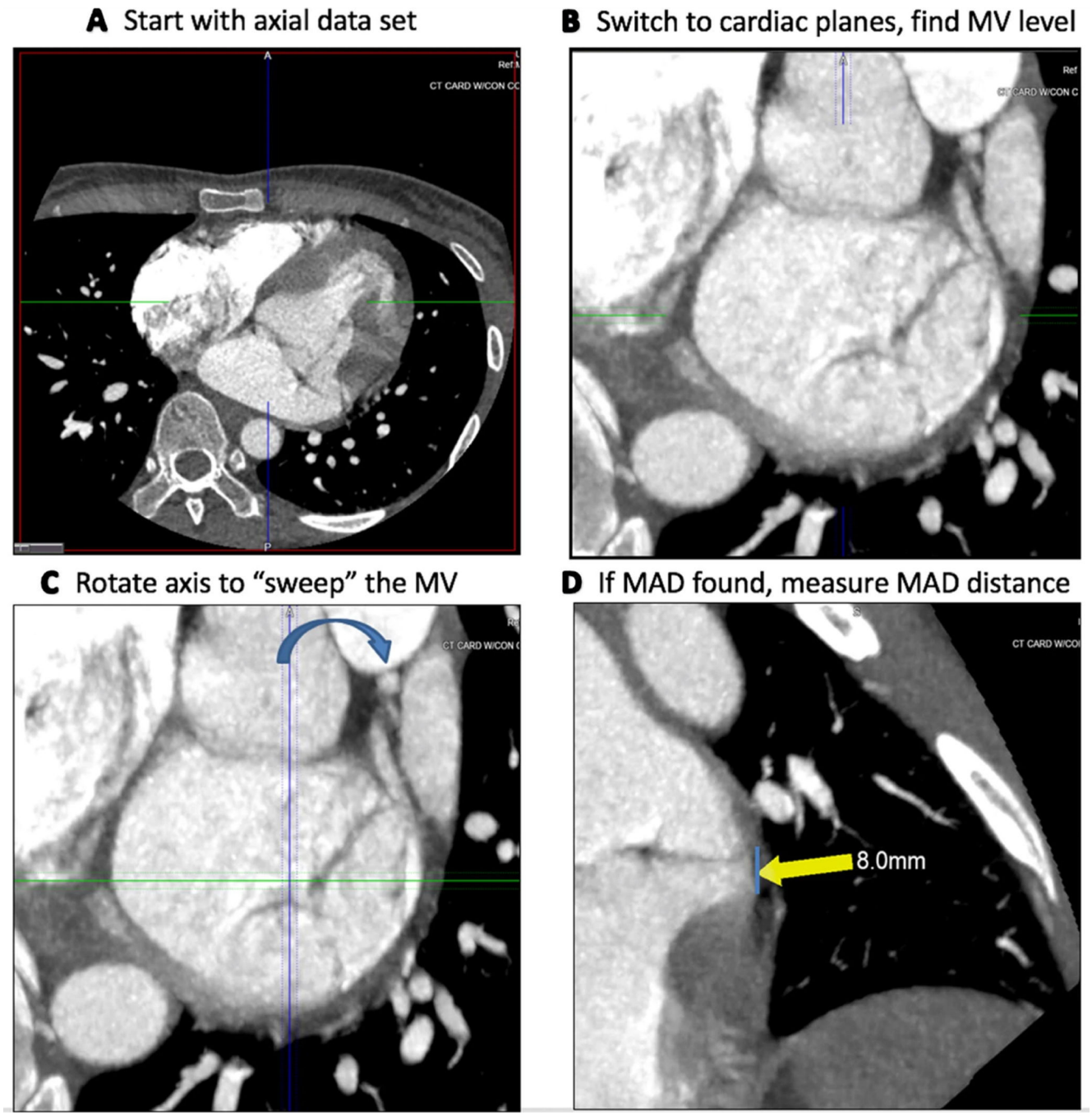

Fig. 3.

Guide for the CT assessment of MAD. End-systolic phase axial images (**a**) are loaded and then converted into "cardiac planes" (**b**). One of the planes going through the mitral valve is rotated (**c**), while the reader assesses the other two imaging planes for the presence of MAD (**d**)

Table 1

Distribution of prolapsed and flail mitral valve scallops in the 18 patients who had MAD

		Prolapse	Flail
Anterior leaflet	A1	2	0
	A2	3	0
	A3	2	0
Posterior leaflet	P1	8	0
	P2	15	2
	P3	5	1

Table 2

Univariate logistic regression of demographic and CT-measured parameters of patients with MVP and severe MR with MAD, compared to those without MAD

	Odds ratio [OR]	95% CI	p value
Age	1.03	[0.95, 1.12]	0.44
Gender (Female)	11.75	[1.38, 99.7]	0.02*
Left ventricular ED volume	1.06	[0.96, 1.17]	0.27
Left ventricular ES volume	0.91	[0.71, 1.16]	0.45
Left atrial volume	0.99	[0.97, 1.02]	0.53
Left ventricular ejection fraction	0.86	[0.55, 1.34]	0.50
Distance between PM (mm)	0.83	[0.62, 1.09]	0.18
Angle between PMs	1.00	[0.93, 1.07]	0.98
ED MV annulus area	0.97	[0.95, 1]	0.045*
ED annulus dimension, AP	1.14	[0.79, 1.66]	0.47
ED annulus dimension, Lateral	1.48	[0.95, 2.31]	0.08
ES MV area	1.02	[0.99, 1.04]	0.14
ES annulus dimension, AP	0.90	[0.68, 1.19]	0.46
ES annulus dimension, Lateral	1.10	[0.8, 1.52]	0.57
Posterior leaflet length	1.39	[1.03, 1.88]	0.03*
Anterior leaflet length	0.89	[0.71, 1.12]	0.32
Atrial arrhythmias	1.45	[0.09, 23.9]	0.79
Premature ventricular contractions	9.63	[0.52, 177]	0.13
Inferior T-wave inversions	0.39	[0.05, 2.87]	0.36
QTc	1.01	[0.98, 1.05]	0.48

ED end-diastolic, *ES* end-systolic, *PM* papillary muscle, *MV* mitral valve, *AP* anterior–posterior, *mL* milliliter, *mm* millimeters, *msec* milliseconds, *QTc* corrected QT-interval